International Journal of Nanomedicine

Dovepress
open access to scientific and medical research

Open Access Full Text Article

ORIGINAL RESEARCH

Interleukin 10-coated nanoparticle systems compared for molecular imaging of atherosclerotic lesions

This article was published in the following Dove Press journal:
International Journal of Nanomedicine
3 September 2014
Number of times this article has been viewed

Gunter Almer[1,*]
Kelli L Summers[1,2,*]
Bernhard Scheicher[2]
Josef Kellner[3]
Ingeborg Stelzer[1]
Gerd Leitinger[4,5]
Anna Gries[3]
Ruth Prassl[6]
Andreas Zimmer[2]
Harald Mangge[1,7]

[1]Clinical Institute of Medical and Chemical Laboratory Diagnostics, Medical University of Graz, Graz, Austria; [2]Institute of Pharmaceutical Sciences, Department of Pharmaceutical Technology, University of Graz, Graz, Austria; [3]Institute of Physiological Chemistry, Medical University of Graz, Graz, Austria; [4]Research Unit Electron Microscopic Techniques, Institute of Cell Biology, Histology and Embryology, Medical University of Graz, Graz, Austria; [5]Center for Medical Research (ZMF), Medical University of Graz, Graz, Austria; [6]Institute of Biophysics, Medical University of Graz, Graz, Austria; [7]BioTechMed, Graz, Austria

*These authors contributed equally to the study

Correspondence: Harald Mangge
Clinical Institute of Medical and Chemical Laboratory Diagnostics, Medical University of Graz, BioTechMed, Auenbruggerplatz 15, 8036 Graz, Austria

Andreas Zimmer
Institute of Pharmaceutical Sciences, Department of Pharmaceutical Technology, University of Graz, BioTechMed, Universitätsplatz 1, 8010 Graz, Austria

Abstract: Atherosclerosis (AS) is one of the leading causes of mortality in high-income countries. Early diagnosis of vulnerable atherosclerotic lesions is one of the biggest challenges currently facing cardiovascular medicine. The present study focuses on developing targeted nanoparticles (NPs) in order to improve the detection of vulnerable atherosclerotic-plaques. Various biomarkers involved in the pathogenesis of atherosclerotic-plaques have been identified and one of these promising candidates for diagnostic targeting is interleukin 10 (IL10). IL10 has been shown to be a key anti-inflammatory responding cytokine in the early stages of atherogenesis, and has already been used for therapeutic interventions in humans and mice. IL10, the targeting sequence, was coupled to two different types of NPs: protamine-oligonucleotide NPs (proticles) and sterically stabilized liposomes in order to address the question of whether the recognition and detection of atherosclerotic-lesions is primarily determined by the targeting sequence itself, or whether it depends on the NP carrier system to which the biomarker is coupled. Each IL10-targeted NP was assessed based on its sensitivity and selectivity toward characterizing atherosclerotic-plaque lesions using an apolipoprotein E-deficient mouse as the model of atherosclerosis. Aortas from apolipoprotein E-deficient mice fed a high fat diet, were stained with either fluorescence-labeled IL10 or IL10-coupled NPs. Ex vivo imaging was performed using confocal laser-scanning microscopy. We found that IL10-targeted proticles generated a stronger signal by accumulating at the surface of atherosclerotic-plaques, while IL10-targeted, sterically stabilized liposomes showed a staining pattern deeper in the plaque compared to the fluorescence-labeled IL10 alone. Our results point to a promising route for enhanced in vivo imaging using IL10-targeted NPs. NPs allow a higher payload of signal emitting molecules to be delivered to the atherosclerotic-plaques, thus improving signal detection. Importantly, this allows for the opportunity to visualize different areas within the plaque scenario, depending on the nature of the applied nanocarrier.

Keywords: interleukin 10, atherosclerotic plaques, nanoparticles, proticles, liposomes

Introduction

Despite considerable therapeutic advances over the past 50 years, cardiovascular events are the leading cause of death worldwide. This is primarily due to the increasing prevalence of atherosclerosis (AS).[1,2] AS is defined as a sub-acute inflammatory vascular disease, characterized by both lipid deposits and the infiltration of macrophages and T-cells which interact both with one another and with arterial vessel wall cells.[3,4] Currently, only advanced-stage AS can be diagnosed – either by directly measuring the degree of stenosis or by evaluating the effect of arterial stenosis on organ perfusion.[5,6] A reliable, non-invasive imaging technique that detects early-stage atherosclerotic-plaques, and, more importantly, the vulnerable plaques leading to cardiovascular

events, is a crucial stepping stone in addressing the current atherosclerosis epidemic.[7]

Interleukin 10 (IL10), a type II cytokine, is the most prominent anti-inflammatory cytokine.[8] It plays a key role in counter-regulating the immune and inflammatory responses in AS pathogenesis by inhibiting the production of pro-inflammatory cytokines and mediators from macrophages and dendritic cells.[9–12] The comparatively high amounts of IL10 found in atherosclerotic-plaques make it diagnostically relevant.[13,14] IL10 is produced by a variety of sources which include, but are not limited to, T-helper cells,[15] monocytes, macrophages,[9] epithelial cells, and tumor cells.[16,17] Recombinant IL10 has already been used in humans for therapeutic interventions.[18] A study by Chernoff et al showed that IL10 is well tolerated without serious side effects at doses of up to 25 μg/kg.[18] It has also been shown that treatment with IL10 inhibits the development of type I diabetes mellitus in non-obese diabetic mice.[19] From a design standpoint, IL10 has the potential to be dually used as a biomarker for diagnosis and a therapeutic agent.

Recently, we have shown that fluorescently-labeled IL10 and IL10-coupled liposomes can detect atherosclerotic-plaques in apolipoprotein E (ApoE)-deficient mice. Therefore, we aim to exploit the binding affinity of IL10 to atherosclerotic-lesions by using it as the targeting sequence for two different types of nanoparticles (NPs).

We began by examining protamine-oligonucleotide (ON) NPs, known as proticles. Proticles are biodegradable NPs which were developed and characterized by our group in the delivery of various active compounds such as antisense ONs or small peptides.[20–23] Proticles are formed by the spontaneous self-assembly of oppositely-charged biomolecules (protamine and ONs) in an aqueous solution. Once formed, proticles can also be coated with targeting sequences.[24]

Next, we tested sterically stabilized liposomes which are frequently used as drug delivery systems and increasingly for targeted imaging.[25–27] Liposomes provide several advantages as an NP carrier system: 1) they are easily made using a flexible set of lipid building blocks; 2) they are highly biocompatible and exhibit favorable prolonged residence times in circulation when prepared with polymer grafts;[28,29] and 3) they are reported to be non-immunogenic.[30,31] Different imaging modalities can detect liposomes after a simple modification using signal-emitting particles. Additionally, functionalized groups with specific antibodies or proteins can be attached to the distal end of the liposome's polyethylene glycol (PEG)-chains – ultimately enabling specific cells to recognize this NP carrier system.[26,27,32]

Both the proticle and liposome NPs can be loaded with numerous signal-emitting molecules (ie, fluorescent molecules). Thus, we expected a brighter signal within atherosclerotic-plaque areas using the NPs as compared to only using labeled IL10 which only has two fluorescent molecules per IL10 protein. To test this hypothesis, we coupled IL10 to the two NPs mentioned previously, and then, with confocal laser scanning microscopy, monitored the ability of these IL10-targeted NPs to recognize, bind, and accumulate in the aortic atherosclerotic-plaques of ApoE-deficient mice.

Materials and methods

Materials

Recombinant murine IL10 expressed in *Escherichia coli* was purchased from GenScript, Inc., (Piscataway, NJ, USA) and later from PeproTech (Rocky Hill, NJ, USA).

The proticles were made from the self-assembly of protamine free base and ONs with a non-coding, random sequence (5′-ACG TTG GTC CTG CGG GAA-3′). The protamine free base was obtained from Sigma-Aldrich Co. (St Louis, MO, USA), and the ONs were obtained from Biospring GmbH (Frankfurt, Germany).

To achieve fluorescent imaging, a defined fraction of unlabeled protamine was replaced with rhodamine-red-mal-protamine, which was synthesized by piChem (Graz, Austria). For the liposomes, palmitoyl-oleoyl-phosphatidylcholine, polyethylene glycol conjugated distearyl-phosphatidylethanolamine (DSPE-PEG2000), cholesterol, and the functionalized lipid 1,2-dipalmitoyl-sn-glycero-3-phosphothioethanol were purchased from Avanti Polar Lipids (Alabaster, AL, USA). The remaining materials, 3-(N-succinimidyloxyglutaryl) (NHS) aminopropyl polyethylene glycol-carbamyldistearoylphosphatidyl-ethanolamine (DSPE-PEG-NHS, PEG-chain MW =2000), were obtained from NOF America Corporation (White Plains, NY, USA).

The long wavelength-emitting dye, Atto655 (ATTO-TEC GmbH, Siegen, Germany) was used as amine reactive carboxylic acid succinimidyl ester (Atto655-NHS) for IL10 labeling, while the maleimide-functionalized dye Atto655-Mal was covalently coupled to 1,2-dipalmitoyl-sn-glycero-3-phosphothioethanol to label liposomes. Labeling procedures were performed as described previously.[33] Water for all NP preparations (Milli-Q; Millipore; Vienna, Austria) was purified with a Milli-QPlus gradient system from EMD Millipore (Billerica, MA, USA). All other chemicals were analytical grade.

Recombinant mouse IL10 was detected by Western blot (WB) using the SuperSignal® West Femto maximum sensitivity substrate kit (Thermo Fisher Scientific, Waltham, MA, USA). For this, a primary monoclonal

rabbit anti-human IL10 antibody (Epitomics, Burlingame, CA, USA) was used in combination with a horse radish peroxidase (HRP)-conjugated secondary goat anti-rabbit antibody.

AlexaFluor488 pre-labeled rat anti-mouse CD68 antibody was used as a macrophage marker; CD31 antibody was used as an endothelial cell marker; and an unspecific rat anti-human immunoglobulin G2a was used as the negative control. These were all purchased from AbD Serotec (Kidlington, UK).

Preparation of uncoated and IL10-coated proticles

The strong ionic interactions between positively charged protamine and negatively charged ON are the basis for proticle formation. The components self-assemble within the first few seconds of being mixed in an aqueous solution, as previously described.[34] The composition of the proticles is given as a mass ratio between the components, referring to a constant protamine concentration of 100 μg/mL. Using fluorescent microscopy, an optimal fluorescent signal was determined to be a 10% replacement of protamine with rhodamine-red labeled protamine. Proticles were assembled by combining the protamine/rhodamine-red-mal-protamine mixture with the ON solution followed by 5 minutes of incubation. For IL10 coating, preassembled proticles were mixed with an IL10 solution and then incubated for 1 hour at room temperature on an orbital shaker (150 rpm). IL10-coated proticles were achieved using a final IL10 concentration 20-, 200-, and 20,000-fold lower than the protamine concentration.

Preparation of uncoated and IL10-coated stealth liposomes

Liposomes were composed of palmitoyl-oleoyl-phosphatidylcholine/cholesterol/DSPE-PEG2000 functionalized with NHS/DPP-TE-Atto655 dye component at molar ratios of 3/2/0.3/0.01. Liposomes (10 mg/mL phospholipid content) were made using a dry film rehydration technique, followed by size extrusion, as described previously.[35] For IL10 coupling, 45 μg of IL10 was added to 500 μL of pre-formed, extruded liposomes (molar NHS-ester to protein ratio of 200:1) in a 150 mM bicarbonate buffer with a pH of 8.2 and then incubated overnight at room temperature under constant, slight agitation. The reaction was stopped by adding a 10-fold molar excess, with respect to NHS-ester, of 2-aminoethanol. The blocking agent and non-bound protein were removed by extensive dialysis against 10 mM phosphate buffered saline (PBS) (pH 7.4), using a dialysis membrane with a cut-off of 50 kDa.

NP characterization

Mean particle size of both NP systems (hydrodynamic diameter, Z-Average), size distribution (polydispersity index, PDI) and zeta potential (electrophoretic mobility) were measured with a Zetasizer Nano ZS (Malvern Instruments, Malvern, UK). Samples were diluted with Milli-Q water (Millipore) and the measurements were carried out at 25°C. Probes were measured as IL10-coated and non-coated NPs.

Both the amount of protamine incorporated into the NPs and the IL10 coating efficiency were determined by an indirect quantification method. After preparation, proticle dispersion was centrifuged at 14,000 rpm, 4°C for 2 hours (Eppendorf centrifuge 5,804 R; Eppendorf, Hamburg, Germany), and then the collected supernatant was centrifuged for 2 hours. Afterwards, the concentration of protamine or IL10 in the supernatant was determined. Protamine was quantified via reversed phase, high performance liquid chromatography using a water/acetonitrile (both 0.075% trifluoracetic acid volume/volume) gradient system (95:5 to 10:90 within 25 minutes, 1 mL/min, detection at 215 nm) equipped with a Zorbax 300Extend-C18, 4.6×100 mM column (Agilent Technologies, Santa Clara, CA, USA) and a Merck-Hitachi HPLC system (EMD Millipore). The concentration of IL10 was determined with an enzyme-linked immunosorbent assay (ELISA, BioLegend, Inc, San Diego, CA, USA), and absorbance values were analyzed with a ultraviolet/visible/fluorescent plate reader (Fluostar Galaxy; BMG Labtech, Ortenberg, Germany).

The binding affinity of IL10 to liposomes was quantified with the same ELISA system that was used for the IL10-proticles. A qualitative proof for coupling was performed with native polyacryl amide gel electrophoresis (PAGE) followed by WB analysis. After fluorescence imaging of the labeled proteins excited at λ_{flu} =750 nm (Maestro In Vivo Imaging System™, CRi, Woburn, MA, USA), the gels were control stained with Bio-Safe™ Coomassie G250 stain (Bio-Rad Laboratories Inc., Hercules, CA, USA). For Western blotting, the samples from the unstained precast gels were blotted to polyvinylidene difluoride membranes with 120 V for 1 hour at 4°C. Immunoblots were blocked and incubated with a primary anti-IL10 Ab (200 ng/mL); each step was taken overnight at 4°C. Then the immunoblots were detected with a secondary Ab (4 ng/mL), and visualized by a chemiluminescence reaction using the SuperSignal® West Femto maximum sensitivity substrate kit. The shape and morphology of IL10-coated liposomes was assessed by electron microscopy. Transmission electron microscopic images were recorded using a Zeiss EM 902 electron microscope, operating at an acceleration

voltage of 50 kV. Briefly, 4 µL of the liposomal suspensions were applied to a carbon-over-Pioloform-coated grid and incubated for one minute. Any excess was soaked up with filter paper and replaced immediately with 4 µL of uranyl acetate-solution (1% in double distilled water). Samples were incubated for 1 minute, blotted, air dried, and viewed at a magnification of 30,000.

Animal experiments

All animal procedures were approved by the Austrian Ministry of Science and Research. Two to four month old ApoE-deficient mice with a C57BL/6J genetic background (Charles River Laboratories, Belgium) were fed a Western Type Diet (21% XL) of experimental food (Ssniff, Germany) for 2–3 months. At least three mice were used for each staining trial. All experiments were performed independent of sex. An injured endothelium was defined as an activated endothelial layer covering the atherosclerotic lesions of ApoE-deficient mice. For each ex vivo staining trial, mice were randomly sacrificed with an overdose of isoflurane (Abbott Laboratories, Abbott Park, IL, USA), the chest was opened and the heart was immediately injected with PBS (pH 7.4) for 15 minutes to rinse the circulation. Finally, the vena cava was excised. The aorta, including the aortic arch, was dissected, cut open, washed with PBS (pH 7.4), and incubated in Krebs-Henseleit solution (118 mM NaCl; 25 mM $NaHCO_3$; 2, 8 mM $CaCl_2$ 2 H_2O; 1, 17 mM $MgSO_4$ 7 H_2O; 4, 7 mM KCl; 1, 2 mM KH_2PO_4; 2 mg/mL glucose; pH 7.4) to sustain its physiological activity while blocking unspecific binding reactions with 1% bovine serum albumin (Sigma-Aldrich Co.) for 1 hour at room temperature. Following this, the samples were incubated with either the fluorescence-labeled biomarker (10 µg/mL of Atto655 labeled IL10) or IL10-coated NPs (2 mg/mL Atto655-labeled IL10-coated stealth liposomes, Atto655-labeled stealth liposomes for negative control; 100 µg/mL rhodamine-labeled IL10-coated proticles or rhodamine-labeled proticles [Rho-proticles] for negative control) for 1–2 hours at 37°C while being shaken in the dark to avoid fluorochrome bleaching. During the last 45 minutes of incubation, the samples were co-stained with either 5 µg/mL of an anti-CD68 pre-labeled antibody to visualize monocyte-derived macrophages or an anti-CD31 antibody to detect the aortic endothelium. Hoechst 33,342 fluorescence dye (1 µg/mL, Thermo Fisher Scientific) was added 10 minutes before the end of the incubation time to stain the cell nuclei. Subsequently, the aortic sections were washed four times in PBS (pH 7.4), placed on a glass slide, covered with polyvinyl alcohol mounting medium containing 1,4-diazabicyclo(2,2,2) octane (DABCO; Sigma-Aldrich Co.), adjusted under a stereo microscope, and squeezed with a cover slip.

Fluorescence imaging by confocal laser-scanning microscopy

At least five to six atherosclerotic-plaques were found on the aortic section of each mouse and then analyzed. The surrounding aortic surface was also included in the analysis. All fluorescence-based and transmitted light images of the sections (Z-Stack images) were acquired with the LSM 510 META Axiovert 200M Zeiss confocal system (Carl Zeiss Meditec AG, Jena, Germany). Images were generated with a 40× Plan-Neofluar 1.3 DIC oil immersion objective (Carl Zeiss Meditec AG) and a multitrack configuration. Hoechst, AlexaFluor488, rhodamine, and Atto655 signals were sequentially monitored with band-pass (BP) 420–480, BP 505–550, and BP 679–743 nm filters after excitation with 405, 488, 543, and 633 nm laser lines, respectively. The Zeiss AIM software version 4.2 (Carl Zeiss Meditec AG) was used for the sequential acquisition of all three channels. All confocal images were acquired with a frame size of 512×512 pixels which was then averaged three times.

Results

Characterization of the proticles

Uncoated proticles had a mean hydrodynamic diameter of 108 nm (mass ratio ON:protamine, 2:1) and 115 nm (ON:protamine, 1:1). Both mass ratios had a narrow size distribution, as indicated by the low PDI values of approximately 0.1. Proticles with a mass ratio of 2:1 were more negatively charged (–57 mV) than the 1:1 proticles (–30 mV). With the addition of IL10, proticles with a 2:1 mass ratio of ON:protamine only showed a slight increase in hydrodynamic diameter (approximately 12 nm). Furthermore, there was a narrow size distribution and mean zeta potential values of –34.7 (±5.4) mV (ON:protamine:IL10, 2:1:5E-5) and –38 (±1.2) mV (2:1:5E-3). In contrast, proticles with a mass ratio of ON:protamine 1:1 showed a significant increase in size after coating with IL10. All of the data are summarized in Table 1. Using reversed phase, high performance liquid chromatography, no protamine was detected in the supernatants of proticle dispersions. This indicates that the total amount of protamine is assembled within the NPs (data not shown). IL10 coating efficiencies were tested with IL10 concentrations 20-fold (ON:protamine:IL10, 2:1:5E-2) and 200-fold (2:1:5E-3) lower than the protamine concentration (Figure 1A). Coated proticles with a mass ratio of 2:1:5E-3 had an IL10 coating efficiency of 55%±5%, and ones with a mass ratio of 2:1:5E-2 had an efficiency of

Table 1 Dynamic light scattering results for uncoated and IL10-coated proticles and liposomes

Mass ratio		Hydrodynamic diameter (nm)	Polydispersity index	Zeta potential (mV)
ON:protamine	**Mouse IL10**			
[a]Proticles				
2:1	0	108.2 (±14)	0.12 (±0.03)	−56.7 (±3.0)
	5E-5	121.0 (±6.6)	0.10 (±0.02)	−34.7 (±5.4)
	5E-3	122.3 (±6.8)	0.09 (±0.01)	−38.0 (±1.2)
	5E-2	118.8 (±3.9)	0.10 (±0.01)	
1:1	0	114.5 (±12.8)	0.10 (±0.03)	−29.5 (±5.5)
	5E-5	1,550.7 (±737.4)	0.48 (±0.31)	−3.6 (±5.3)
	5E-3	1,551.0 (±1,081.7)	0.54 (±0.47)	−3.0 (±0.9)
	5E-2	417.5 (±234.3)	0.04 (±0.03)	
[b]Liposomes				
Composition (molar lipid ratio)				
POPC:DSPE-PEG2000:cholesterol (3:0.3:2)		150±1.02 (n=5)	0.069±0.01	−19.5±3.6
POPC:DSPE-PEG2000-NHS-IL10:cholesterol (3:0.3:2)		162±0.6 (n=5)	0.065±0.01	−42.8±0.6

Notes: [a]The composition of proticles is given as a mass ratio between the components, with a protamine concentration of 100 µg/mL. Results are given as mean values ± standard deviations from at least eight measurements (hydrodynamic diameter, polydispersity index) and four measurements (zeta potential). [b]Uncoated or IL10-coated liposomes were characterized by the same parameters.

Abbreviations: ON, oligonucleotides; IL10, interleukin 10; POPC, palmitoyl-oleoyl-phosphatidylcholine; DSPE, distearyl-phosphatidylethanolamine; PEG, polyethylene glycol; NHS, N-hydroxysuccinimide.

68%±12%. To achieve the latter efficiency, 500 ng of IL10 was coated onto proticles consisting of 15 µg protamine and 30 µg ON (ON:protamine:IL10, 2:1:5E-2, sample volume 150 µL). Taking into account that 2:1:E-3 and 2:1:E-2 IL10-coated proticles showed similar coating efficiencies, the proticles with the highest concentration of IL10 (mass ratio ON:protamine:IL10, 2:1:5E-2) were selected for the subsequent experiments.

Characterization of liposomes

For the untargeted liposomes, the average particle diameter was 150 nm with a PDI of 0.07. IL10 was coupled to NHS-functionalized liposomes via NHS-ester binding on the surface and the average diameter of coated liposomes was 162 nm with a PDI of 0.06. All the data are summarized in Table 1. The coupling efficiency was determined by an IL10 ELISA. A standard curve of different concentrations of IL10 was compared with untargeted liposomes (negative control) and IL10-targeted liposomes, whereby the amount of NPs was calculated based on the total amount of IL10 used (=9 µg IL10/mg liposomes). The average binding rate of the IL10 to the liposomes was 43%±3.2% (~3.9 µg IL10/mg liposomes). A qualitative analysis of the coupling was performed by native PAGE and WB. Due to the characteristics of the native PAGE, the fluorescence-labeled liposomes are immobilized in the matrix of the gel pockets (Figure 1B, lane 1 and 3). Unspecific Coomassie blue solution stained both IL10- and Atto655-labeled liposomes (see Figure 1C). The WB results then showed that IL10 conjugated to liposomes is also immobilized with the liposomes in the gel slots (see Figure 1D, lane 2). A small amount of unbound IL10 was detected in the native gel by Coomassie staining and by WB. Transmission electron microscopic images of the liposomes revealed spherical particles whose integrity was preserved after ligand coupling (Figure 1E).

Staining of atherosclerotic-plaques with IL10-coated proticles

Aortas dissected from ApoE-deficient mice were incubated with Rho-proticles, since no significant interfering autofluorescent signal was observed for unstained blank sections, as imaged by confocal laser scanning microscopy at λ_{ext} =543 nm. This was observed from both the whole uninjured aortic tissue and the scanned atherosclerotic-plaques (data not shown). To examine any unspecific binding of proticles to the inner aortic surface, the aortic sections were incubated with Rho-proticles as the control. The scans showed a weak accumulation of aggregated proticle spots on the entire aortic surface (Figure 2 and 3A). On the atherosclerotic-plaque areas, however, the staining patterns were slightly stronger and had a more differentiated structure (Figure 2 and 3B). After staining with IL10-Rho-proticles, no significant differences were observed between IL10-Rho-proticles and untargeted Rho-proticles in terms of the staining patterns on the uninjured inner aortic surface (Figure 2 and 3A and C). Still, IL10-Rho-proticles generated a stronger staining signal in atherosclerotic-plaques, as compared to the controls (Figure 2 and 3B and D).

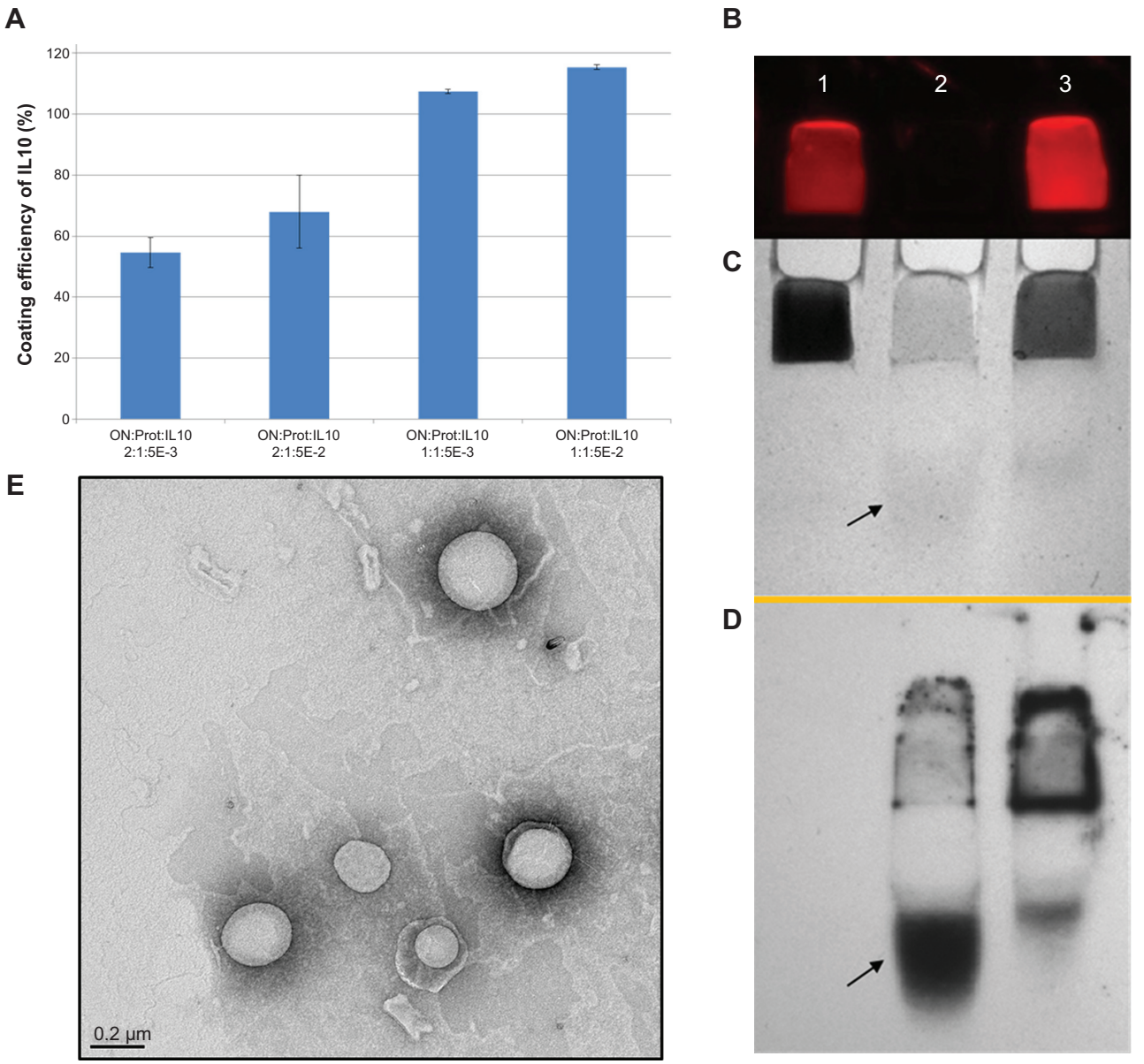

Figure 1 Characterization of IL10 coupled nanoparticles.

Notes: (**A**) Coating efficiency of mouse IL10. Calculation of coating efficiency as the percentage of deployed IL10. Mean values are shown with error bars representing the standard deviation, n=4. Proticles with a mass ratio of 2:1 (ON:protamine) showed similar IL10 coating efficiencies using different IL10 concentrations. For 1:1 proticles, complete binding of IL10 was recorded, but because the proticles aggregated, IL10 was also incorporated between the aggregates, and thus, not solely presented at the surface. (**B**–**D**) IL10-coupled liposomes were applied to a native PAGE gel and then transferred onto a WB membrane. (**B**) Slots of the gel containing the immobilized probes, visualized by fluorescence imaging when excited at λ_{flu} =750 nm. (**C**) The same gel in (**B**), but stained with Coomassie blue protein solution, showing that liposomes are stained by the solution. (**D**) WB membrane of the gel, detected by a primary anti-IL10 Ab and a secondary HRP-conjugated Ab, followed by a substrate reaction and luminescence visualization which shows free and liposomal-bound IL10. Lane 1, Atto655 labeled liposomes; lane 2, native IL10; lane 3, IL10-ATTO655-liposomes after dialysis. Atto655 was purchased from ATTO-TEC GmbH, Siegen, Germany. The arrows show the position of free IL10. (**E**) A representative TEM image illustrates the size distribution and morphology of IL10-coupled liposomes.

Abbreviations: E, exponent – 10^{-3}; ON, oligonucleotides; PAGE, polyacryl amide gel electrophoresis; Prot, protamine; IL10, interleukin 10; HRP, horseradish peroxidase; WB, Western blot; TEM, transmission electron microscopic; Ab, antibody.

Using anti-CD31 co-staining, a strong co-localization of the fluorescent signals was found at the atherosclerotic-plaques (Figure 2D). This suggests that the IL10-Rho-proticles are mainly internalized by the "active, inflammatory" endothelial layer covering the atherosclerotic-plaques.

From the anti-CD68 co-staining, we also found a partial co-localization with IL10-Rho-proticles (Figure 3D), which indicates that proticles are also internalized, most probably by macrophages.

Staining of atherosclerotic-plaques with IL10-coated stealth liposomes

As shown in our previous work, no significant interfering autofluorescent signals were observed at λ_{ext} =633 nm for

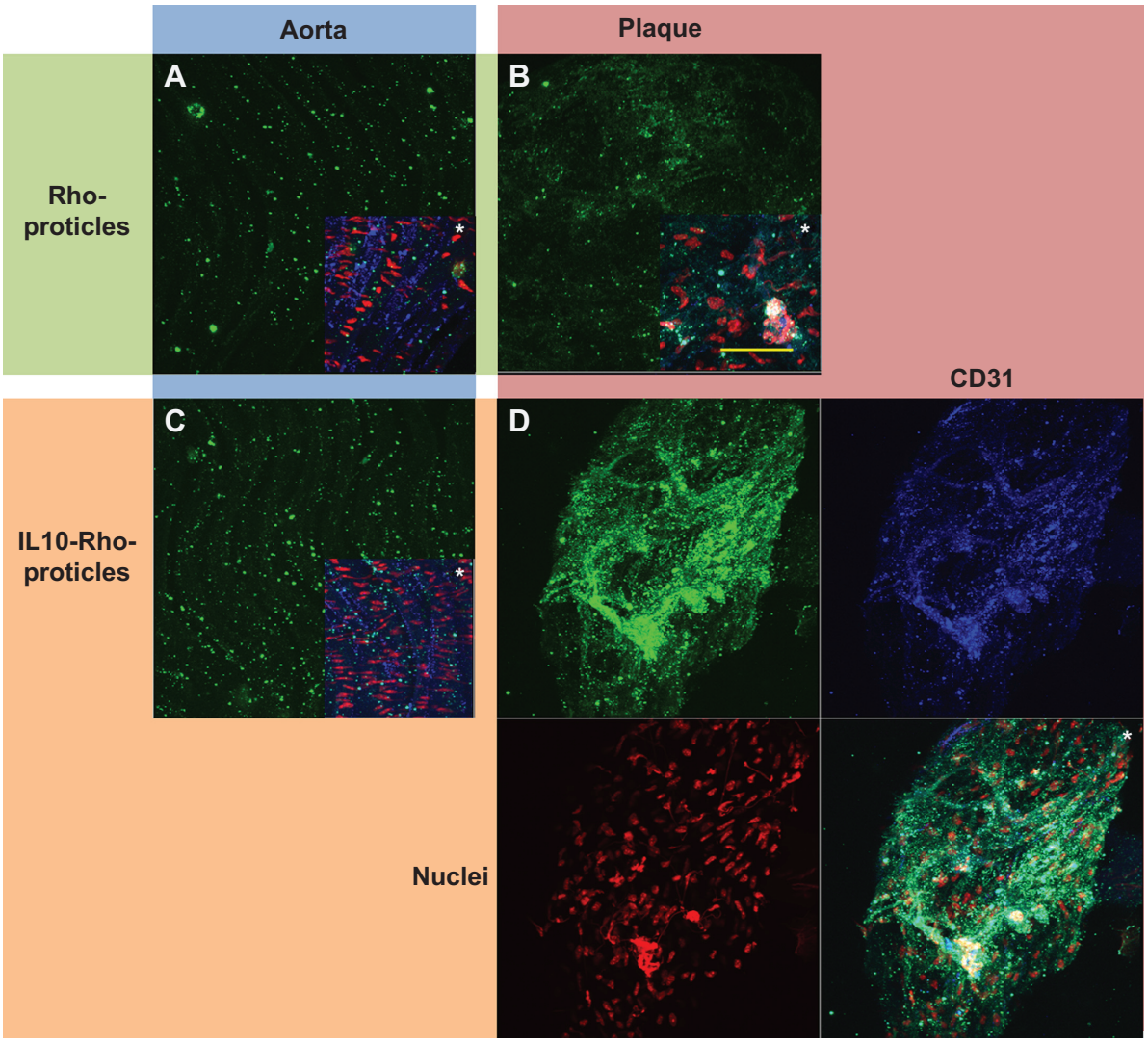

Figure 2 The staining signal of IL10-coated protamine- and oligonucleotide-based NPs, detected on atherosclerotic-plaques and compared to controls.
Notes: Aortic sections of ApoE-deficient mice were incubated with rhodamine-labeled proticles for control (**A**) and (**B**), or coated with IL10 (**C**) and (**D**); NP signals are shown in green. Less-injured aortic areas are shown in (**A**) and (**C**) (blue area), atherosclerotic-plaques in (**B**) and (**D**) (red area). All images are depicted merged (*) with co-stainings for CD31 (endothelium) shown in blue and for the nuclei shown in red; images of the IL10-Rho-proticles stained plaque are also shown split. IL10-Rho-proticles were found to highly co-localized with the endothelium of atherosclerotic-plaques (bluish-green color). Bar indicates 50 μm.
Abbreviations: IL10, interleukin 10; NPs, nanoparticles; AS, atherosclerotic; ApoE, apolipoprotein E; Rho, rhodamine.

unstained blank sections.[33] After incubating aortic sections from ApoE-deficient mice with untargeted Atto655-liposomes, we found a dotted fluorescent signal pattern on the inner surface, particularly in the plaque regions and in the less-injured surrounding area (Figure 4A and B). A slightly weaker staining pattern was observed with IL10-coated Atto655-liposomes on the uninjured areas of the inner aortic surface (Figure 4C and D) as compared with the untargeted liposomes. In contrast, a strong fluorescent signal was detected from the IL10-Atto655-liposomes at the atherosclerotic-plaques.

Moreover, like the IL10-Rho-proticles, the staining signal of IL10-Atto655-liposomes showed a minor co-localization with CD68-stained monocyte/macrophages, which were detected in the plaque area (Figure 4D).

Discussion

The value of targeted NPs is rising exponentially as modern medicine moves toward a preventative strategy of early detection and medication – NPs are ideal constructs for drug delivery and non-invasive imaging.[36–38] Although cancer therapy and cancer diagnostics still dominate the field, the detection of atherosclerotic-plaques is an equally attractive endeavor because it provides a path to preventing the number one killer worldwide, cardiovascular end points.[5,38,39]

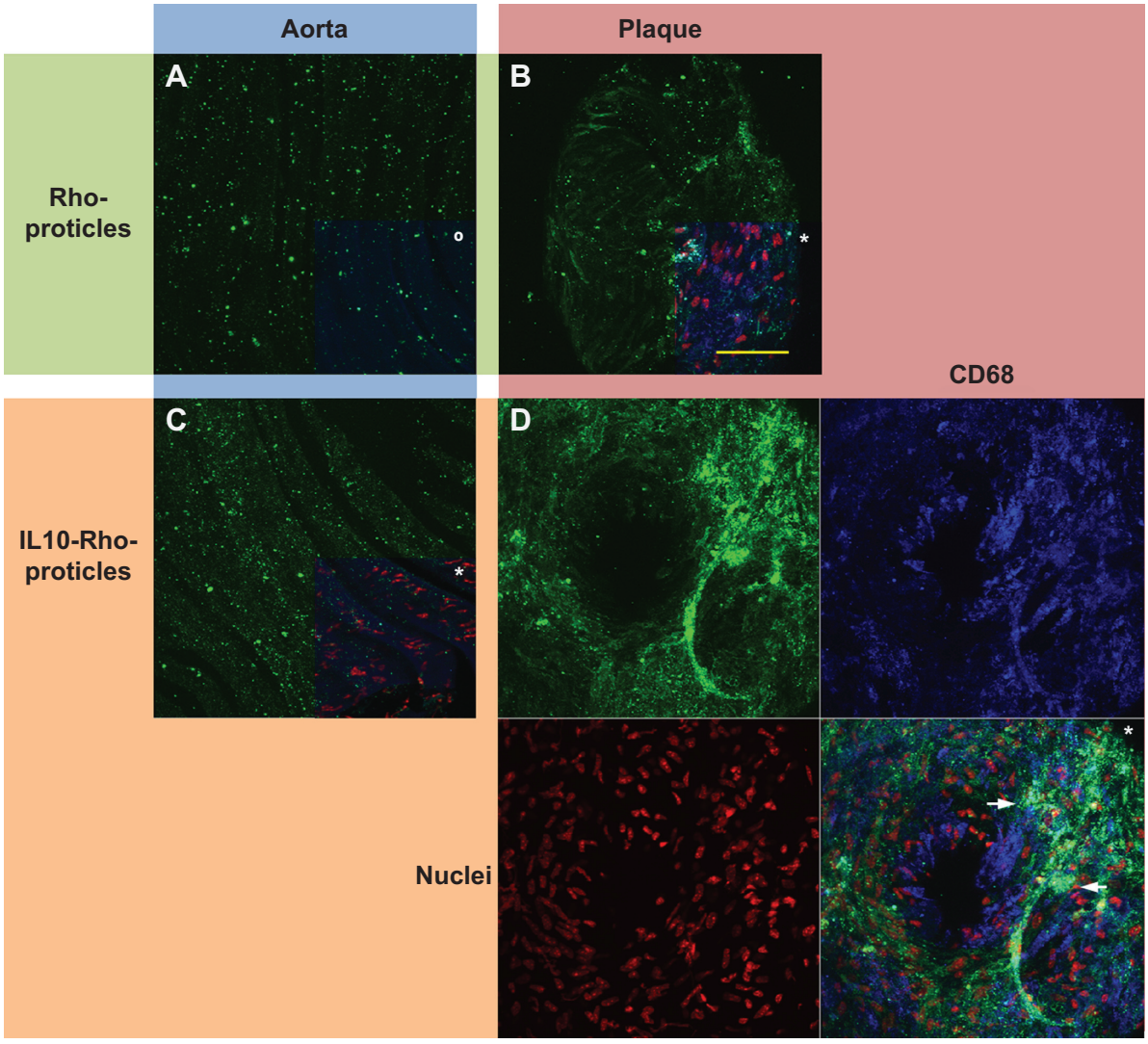

Figure 3 The staining signal of IL10 coated protamine- and oligonucleotide-based NPs, detected on atherosclerotic-plaques and compared to controls.
Notes: Aortic sections of ApoE-deficient mice were incubated with rhodamine-labeled proticles for control (**A**) and (**B**), or coated with IL10 (**C**) and (**D**); NP signals are shown in green. Less-injured aortic areas are shown in (**A**) and (**C**) (blue area), atherosclerotic-plaques in (**B**) and (**D**) (red area). All images are depicted merged with co-stainings for CD68 (macrophages) shown in blue and for the nuclei shown in red (*all; °without nuclei); images of the IL10-Rho-proticles stained plaque are also shown split. IL10-Rho-proticles were found to partially co-localized with CD68 positive macrophages (arrows pointing to the bluish-green color). Bar indicates 50 μm.
Abbreviations: IL10, interleukin 10; NPs, nanoparticles; AS, atherosclerotic; ApoE, apolipoprotein E; Rho, rhodamine.

Atherosclerosis is a chronic disease in which immune-inflammatory processes drive the formation, progression, and rupture of atherosclerotic-plaques.[40] A key event in the AS pathology is the differentiation of monocytes into lesional macrophages and foam cells, a process driven by immune-inflammatory cascades.[4,41] Consequently, several mediators involved in the immune-inflammatory scenario during the progression of AS have been identified and promoted as potential biomarkers to recognize atherosclerotic-lesions.[4,39,42]

We have previously shown that IL10, the anti-inflammatory, "master" cytokine, is also a promising candidate. This biomarker, which targets the thus far neglected anti-inflammatory cascade, is an interesting, and probably even more specific, approach to the molecular imaging of the atherosclerotic-plaque pathogenesis.

In the present study, we chose recombinant IL10 for the targeting sequence. Based on our previous observations,[12] IL10 accumulates in the macrophage-enriched area(s) of atherosclerotic-plaques. By looking toward the future of NPs as transporters of signal-emitting molecules, contrast agents, or drugs, we aimed to assess whether IL10-coupled NPs could produce the necessary signal enhancement for high resolution in vivo detection. We tested two different kinds of NPs, namely stealth liposomes and proticles, in ApoE-deficient mice fed a Western Type Diet.

Liposomes are well-established NPs. Although proticles are less explored, they have nevertheless proven to

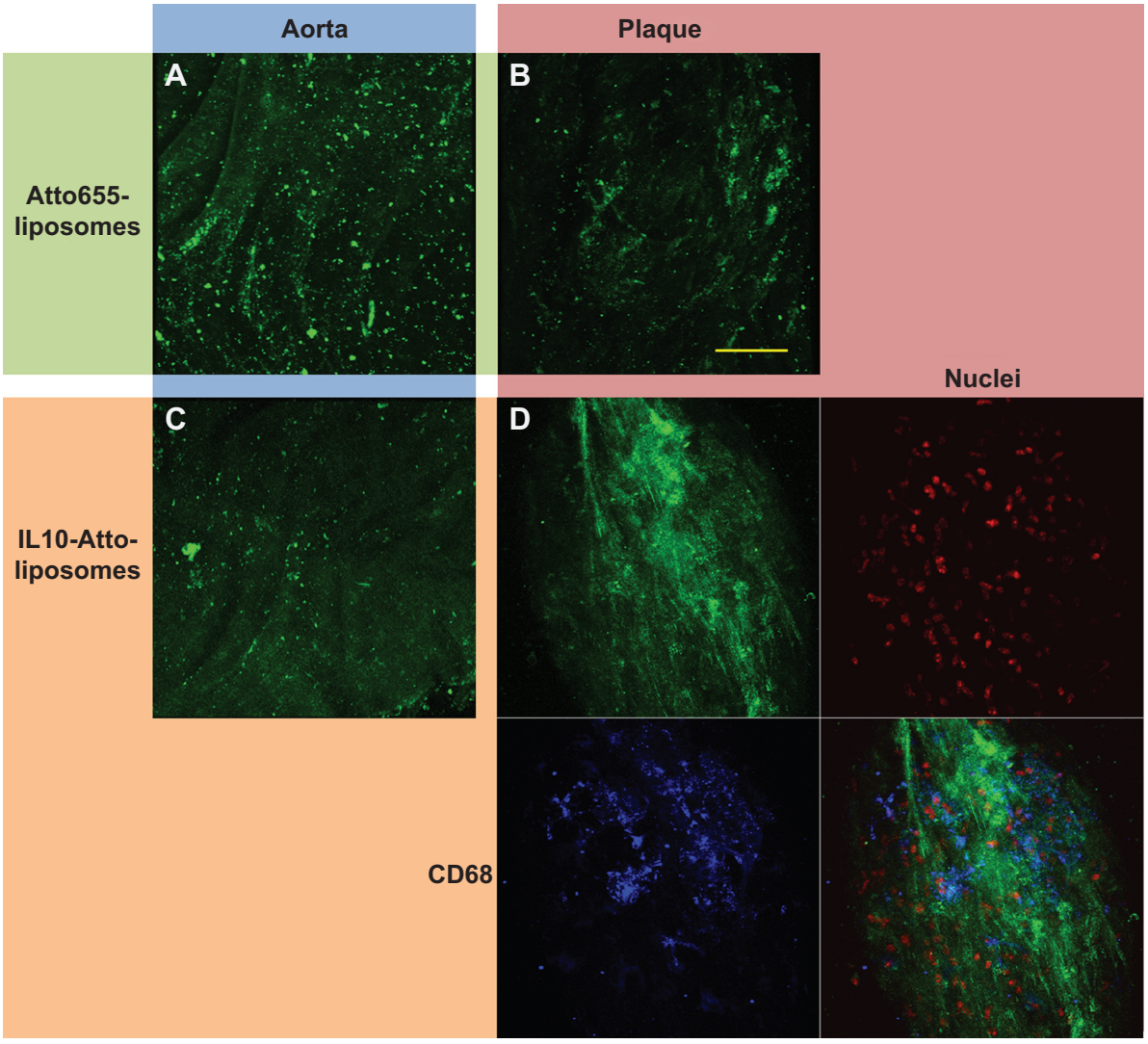

Figure 4 The staining signal of IL10-coated, Atto655 labeled stealth-liposomes, detected on atherosclerotic-plaques and compared to controls.
Notes: Atto655 was purchased from ATTO-TEC GmbH, Siegen, Germany. Aortic sections of ApoE-deficient mice were incubated with Atto655-liposomes as a control (**A**) and (**B**), or coated with IL10 (**C**) and (**D**); NP signals are shown in green. Less-injured aortic areas are shown in (**A**) and (**C**) (blue area) and atherosclerotic-plaques in (**B**) and (**D**) (red area). The image of the IL10-Atto655-liposome stained plaque is depicted with co-stainings for CD68 (macrophages) shown in blue and for the nuclei shown in red. Atto655-liposomes were found to stain the whole aortic sections unspecifically, while IL10-Atto655-liposomes are preferentially accumulated at atherosclerotic-plaque areas. Bar indicates 50 μm.
Abbreviations: IL10, interleukin 10; NP, nanoparticle; ApoE, apolipoprotein E.

be successful in drug targeting. They can be coated with targeting ligands, such as small peptides, but also with larger proteins like apoA-1.[24] In an earlier study, we showed that an apolipoprotein coating of proticles increased their permeability through the blood–brain barrier.[24] Most recently, we investigated the targeting effect of vasoactive intestinal peptide incorporated into the proticle matrix. With this system we have demonstrated an association of proticles on the cell surface in vitro, and a specific localization of proticles onto vasoactive intestinal peptide-receptor-positive lung tumor material ex vivo.[43]

In the present study, both types of NPs were coated with the same targeting sequence either by covalent attachment of IL10 to the PEG-spacer on the surface of liposomes or electrostatically bound to the surface of proticles. A comparably large amount of IL10 was attached to the nanocarriers, corresponding to about 11 ng IL10 per 1 μg proticles or, on average, 4 ng per 1 μg liposomes. The size of the proticles was approximately 100 nm with a negative zeta potential, while the liposomes were somewhat larger but also had a net negative zeta potential.

During the coupling of IL10 to proticles (ON:protamine 1:1), high PDI values and a neutral zeta potential suggested that aggregation occurred when IL10 was added. Complete binding of IL10 was recorded, but, due to aggregation of the proticles (see Table 1), some IL10 was also incorporated

between the aggregates, and therefore, was not completely present at the surface. On the contrary, a slight increase in hydrodynamic diameter and low PDI values for coated proticles (ON:protamine 2:1) showed that no aggregation occurred after IL10 addition, and therefore, IL10 is more likely to be located at the surface.

To study the potential for molecular imaging, we performed confocal laser-scan fluorescence microscopy to evaluate the efficiency of the targeted nanocarriers to atherosclerotic-plaques ex vivo. As a negative control, aortic sections of ApoE-deficient mice were stained with Atto655 labeled unspecific rat immunoglobulin G (IgG). Only traces of unspecific IgG accumulation on the atherosclerotic-plaques were detected (data not shown).

We have previously shown that Atto655-IL10 penetrates deep into the plaques when liposomes were the nanocarrier[12] (see also in Figure 5A and B). Upon switching the NP to IL10-coated proticles and comparing all formulations, we observed a different staining pattern where the signal originated more on the surface of the atherosclerotic-plaques (Figure 5C) and strongly co-localized with the endothelium (Figure 2D) and partially with CD68-positive macrophages on the plaque surface (Figure 3D). Thus, the co-localization between IL10-Rho-proticles and anti-CD68 was more intense than that of Atto655-IL10 or IL10-Atto655-liposomes. This observation correlates with the fact that proticles are, in general, more likely to be taken up by macrophages.[33]

Both types of IL10-targeted NPs led to remarkable signal enhancement in atherosclerotic-plaques, as compared to free IL10, untargeted proticles, and untargeted liposomes. Interestingly, the two types of targeted NPs demonstrated quite distinct differences in their binding/internalization behavior. This finding allows the possibility of future plaque characterization by imaging to be entertained.

In addition to chemical composition, particle size, and morphology, zeta potential is an important parameter influencing

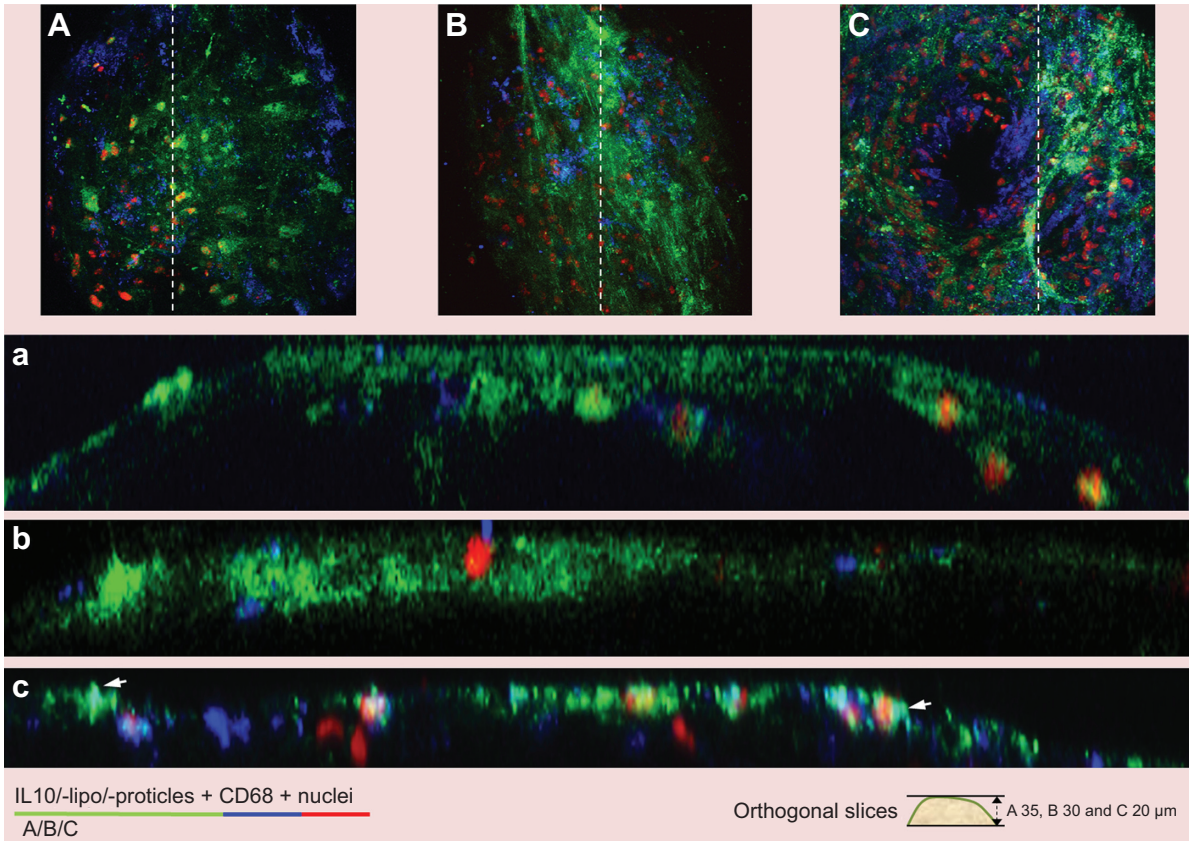

Figure 5 Plaque imaging of IL10-coupled NPs compared to uncoupled IL10.
Notes: Aortic sections of ApoE-deficient mice were incubated with (**A**) Atto655-labeled IL10, (**B**) IL10-coupled Atto655-labeled liposomes or (**C**) rhodamine-labeled IL10-coated proticles. Atto655 was purchased from ATTO-TEC GmbH, Siegen, Germany. The pictures show vertical fluorescence light images from atherosclerotic-plaques that are similar in size. Aortic sections were co-stained with anti-CD68 for macrophages (shown in blue) and with Hoechst (Thermo Fisher Scientific, Waltham, MA, USA) for nuclei (shown in red). By applying IL10 alone (**a**) the signal was found in deeper areas of the plaques which was comparable to IL10-Atto655-liposomes (**b**) where the signal was more condensed. IL10-Rho-proticles were found to greatly accumulate at the plaque surface area; arrows point to areas of strong co-localization with CD68 positive macrophages (**c**).
Abbreviations: IL10, interleukin 10; NPs, nanoparticles; lipo, Atto655-labeled liposomes; ApoE, apolipoprotein E; Rho, rhodamine.

macromolecule interactions and uptake.[44] In general, the phagocytic activity of macrophages is higher for anionic, than cationic, NPs.[45,46] Neutral NPs showed the lowest uptake in vitro.[47,48] In our study, we used negatively charged proticles and liposomes. After IL10 (isoelectric point of 8.3) coupling, the zeta potential of the proticles was further decreased; in contrast, the negative zeta potential of the liposomes increased. In the case of the liposomes, it could be speculated that the coupling of IL10 to the PEG-chains leads to a covering effect, which increases the negative charge of the particles. Taken together, the observed different interaction mechanisms of the NPs within the plaque could be due to charge dependence.

Nevertheless, similar to free fluorescence-labeled IL10, the negatively charged, sterically stabilized IL10-coated liposomes accumulated deeper in atherosclerotic-plaques. This finding is likely due to the enhanced permeability of atherosclerotic-plaque endothelium, caused by the loss of the endothelial glycocalyx.[49] The targeted liposomes weakly co-localized with the monocytes/macrophages detected by anti-CD68 co-staining. Negatively charged proticles adhered slightly to the topographical surface of the plaques. Notably, this uptake by the endothelium and surface monocytes/macrophages was markedly enhanced by IL10 targeting, as proven by anti-CD31 and anti-CD68 co-staining. In ApoE-/- mice, mainly $Gr1^{+}/Ly6C^{hi}$ monocytes are present.[50] These monocytes were reported to adhere to activated endothelium, infiltrate lesions, and then become AS macrophage effectors.[51] Hence, IL10-targeted proticles represent promising markers for atherosclerotic-plaque surface area imaging, while the IL10-targeted liposomes could be a useful device for targeting deeper layers.

A possible limitation may be that the biological efficacy of IL10-targeted liposomes and proticles is hampered by dissociation and poor shelf life characteristics.[52] In the case of liposomes this can be excluded by the stable covalent binding between IL10 and the NP. With regard to proticles, the electrostatic binding of IL10 is usually also stable, whereas behavior under physiologic conditions (eg, blood stream) remains to be seen. Nevertheless, within this study the positive binding in plaques after injection indicates sustained stability during blood transport. The approximate 3–4 week shelf life stability of both proticles and liposomes was found to be adequate.

Conclusion

Taken together, our results demonstrate the potential of two different NPs both targeted with IL10 for the differential recognition of distinct areas within atherosclerotic-lesions. Beyond the diagnostic potential, this also has therapeutic potential because IL10 acts as an anti-inflammatory cytokine.

Hence, the combination of different NPs targeted with the same biomarker may offer new avenues to characterize the inflammatory scenario of atherosclerotic-plaques, or even to discriminate between stable and vulnerable lesions.

Acknowledgments

The study was carried out with financial support from the Commission of the European Communities, under the specific RTD program NanoAthero, grant agreement number NMP4-LA-2012-309820. Special thanks goes to: Matthias Saaba-Lepek, Sandra Falk, and Caroline Vonach for their technical experience and practical contribution.

Disclosure

The authors have no conflict of interest to disclose.

References

1. Tehrani DM, Seto AH. Third universal definition of myocardial infarction: update, caveats, differential diagnoses. *Cleve Clin J Med*. 2013;80(12):777–786.
2. Jneid H, Alam M, Virani SS, Bozkurt B. Redefining myocardial infarction: what is new in the ESC/ACCF/AHA/WHF Third Universal Definition of myocardial infarction? *Methodist Debakey Cardiovascular J*. 2013;9(3):169–172.
3. Rocha VZ, Libby P. Obesity, inflammation, and atherosclerosis. *Nat Rev Cardiol*. 2009;6(6):399–409.
4. Mangge H, Almer G, Truschnig-Wilders M, Schmidt A, Gasser R, Fuchs D. Inflammation, adiponectin, obesity and cardiovascular risk. *Curr Med Chem*. 2010;17(36):4511–4520.
5. Sanz J, Fayad ZA. Imaging of atherosclerotic cardiovascular disease. *Nature*. 2008;451(7181):953–957.
6. Helft G, Worthley SG, Fuster V, et al. Progression and regression of atherosclerotic lesions: monitoring with serial noninvasive magnetic resonance imaging. *Circulation*. 2002;105(8):993–998.
7. Camici PG, Rimoldi OE, Gaemperli O, Libby P. Non-invasive anatomic and functional imaging of vascular inflammation and unstable plaque. *Eur Heart J*. 2012;33(11):1309–1317.
8. Commins S, Steinke JW, Borish L. The extended IL-10 superfamily: IL-10, IL-19, IL-20, IL-22, IL-24, IL-26, IL-28, and IL-29. *J Allergy Clin Immunol*. 2008;121(5):1108–1111.
9. de Waal Malefyt R, Abrams J, Bennett B, Figdor CG, de Vries JE. Interleukin 10 (IL-10) inhibits cytokine synthesis by human monocytes: an autoregulatory role of IL-10 produced by monocytes. *J Exp Med*. 1991;174(5):1209–1220.
10. Peguet-Navarro J, Moulon C, Caux C, Dalbiez-Gauthier C, Banchereau J, Schmitt D. Interleukin-10 inhibits the primary allogeneic T-cell response to human epidermal Langerhans cells. *Eur J Immunol*. 1994;24(4):884–891.
11. Fiorentino DF, Zlotnik A, Mosmann TR, Howard M, O'Garra A. IL-10 inhibits cytokine production by activated macrophages. *J Immunol*. 1991;147(11):3815–3822.
12. Almer G, Frascione D, Pali-Scholl I, et al. Interleukin-10: an anti-inflammatory marker to target atherosclerotic lesions via PEGylated liposomes. *Mol Pharm*. 2013;10(1):175–186.
13. Mallat Z, Heymes C, Ohan J, Faggin E, Leseche G, Tedgui A. Expression of interleukin-10 in advanced human atherosclerotic plaques: relation to inducible nitric oxide synthase expression and cell death. *Arterioscler Thromb Vasc Biol*. 1999;19(3):611–616.
14. Nishihira K, Imamura T, Yamashita A, et al. Increased expression of interleukin-10 in unstable plaque obtained by directional coronary atherectomy. *Eur Heart J*. 2006;27(14):1685–1689.

15. O'Garra A, Vieira P. T(H)1 cells control themselves by producing interleukin-10. *Nat Rev Immunol*. 2007;7(6):425–428.
16. Moore KW, de Waal Malefyt R, Coffman RL, O'Garra A. Interleukin-10 and the interleukin-10 receptor. *Annu Rev Immunol*. 2001;19:683–765.
17. Williams LM, Ricchetti G, Sarma U, Smallie T, Foxwell BM. Interleukin-10 suppression of myeloid cell activation – a continuing puzzle. *Immunology*. 2004;113(3):281–292.
18. Chernoff AE, Granowitz EV, Shapiro L, et al. A randomized, controlled trial of IL-10 in humans. Inhibition of inflammatory cytokine production and immune responses. *J Immunol*. 1995;154(10):5492–5499.
19. Goudy K, Song S, Wasserfall C, et al. Adeno-associated virus vector-mediated IL-10 gene delivery prevents type 1 diabetes in NOD mice. *Proc Natl Acad Sci U S A*. 2001;98(24):13913–13918.
20. Junghans M, Kreuter J, Zimmer A. Antisense delivery using protamine-oligonucleotide particles. *Nucleic Acids Res*. 2000;28(10):E45.
21. Lochmann D, Weyermann J, Georgens C, Prassl R, Zimmer A. Albumin-protamine-oligonucleotide nanoparticles as a new antisense delivery system. Part 1: physicochemical characterization. *Eur J Pharm Biopharm*. 2005;59(3):419–429.
22. Weyermann J, Lochmann D, Georgens C, Zimmer A. Albumin-protamine-oligonucleotide-nanoparticles as a new antisense delivery system. Part 2: cellular uptake and effect. *Eur J Pharm Biopharm*. 2005;59(3):431–438.
23. Wernig K, Griesbacher M, Andreae F, et al. Depot formulation of vasoactive intestinal peptide by protamine-based biodegradable nanoparticles. *J Control Release*. 2008;130(2):192–198.
24. Kratzer I, Wernig K, Panzenboeck U, et al. Apolipoprotein A-I coating of protamine-oligonucleotide nanoparticles increases particle uptake and transcytosis in an in vitro model of the blood–brain barrier. *J Control Release*. 2007;117(3):301–311.
25. Briley-Saebo KC, Mulder WJ, Mani V, et al. Magnetic resonance imaging of vulnerable atherosclerotic plaques: current imaging strategies and molecular imaging probes. *J Magn Reson Imaging*. 2007;26(3):460–479.
26. Erdogan S. Liposomal nanocarriers for tumor imaging. *J Biomed Nanotechnol*. 2009;5(2):141–150.
27. Cormode DP, Skajaa T, Fayad ZA, Mulder WJ. Nanotechnology in medical imaging: probe design and applications. *Arterioscler Thromb Vasc Biol*. 2009;29(7):992–1000.
28. Immordino ML, Dosio F, Cattel L. Stealth liposomes: review of the basic science, rationale, and clinical applications, existing and potential. *Int J Nanomedicine*. 2006;1(3):297–315.
29. Samad A, Sultana Y, Aqil M. Liposomal drug delivery systems: an update review. *Curr Drug Deliv*. 2007;4(4):297–305.
30. Harding JA, Engbers CM, Newman MS, Goldstein NI, Zalipsky S. Immunogenicity and pharmacokinetic attributes of poly(ethylene glycol)-grafted immunoliposomes. *Biochim Biophys Acta*. 1997;1327(2):181–192.
31. Woodle MC. Controlling liposome blood clearance by surface-grafted polymers. *Adv Drug Deliv Rev*. 1998;32(1–2):139–152.
32. Kelly C, Jefferies C, Cryan SA. Targeted liposomal drug delivery to monocytes and macrophages. *J Drug Deliv*. 2011;2011:727241.
33. Almer G, Wernig K, Saba-Lepek M, et al. Adiponectin-coated nanoparticles for enhanced imaging of atherosclerotic plaques. *Int J Nanomedicine*. 2011;6:1279–1290.
34. Kaul P, Douglas PS. Atherosclerosis imaging: prognostically useful or merely more of what we know? *Circ Cardiovasc Imaging*. 2009;2(2):150–160.
35. Stark B, Debbage P, Andreae F, Mosgoeller W, Prassl R. Association of vasoactive intestinal peptide with polymer-grafted liposomes: structural aspects for pulmonary delivery. *Biochim Biophys Acta*. 2007;1768(3):705–714.
36. Wickline SA, Neubauer AM, Winter PM, Caruthers SD, Lanza GM. Molecular imaging and therapy of atherosclerosis with targeted nanoparticles. *J Magn Reson Imaging*. 2007;25(4):667–680.
37. Choudhury RP, Fisher EA. Molecular imaging in atherosclerosis, thrombosis, and vascular inflammation. *Arterioscler Thromb Vasc Biol*. 2009;29(7):983–991.
38. Lindsay AC, Choudhury RP. Form to function: current and future roles for atherosclerosis imaging in drug development. *Nat Rev Drug Discov*. 2008;7(6):517–529.
39. Nahrendorf M, Sosnovik DE, Weissleder R. MR-optical imaging of cardiovascular molecular targets. *Basic Res Cardiol*. 2008;103(2):87–94.
40. Libby P, Okamoto Y, Rocha VZ, Folco E. Inflammation in atherosclerosis: transition from theory to practice. *Circ J*. 2010;74(2):213–220.
41. Woollard KJ, Geissmann F. Monocytes in atherosclerosis: subsets and functions. *Nat Rev Cardiol*. 2010;7(2):77–86.
42. Mangge H, Almer G, Haj-Yahya S, et al. Preatherosclerosis and adiponectin subfractions in obese adolescents. *Obesity (Silver Spring)*. 2008;16(12):2578–2584.
43. Ortner A, Wernig K, Kaisler R, et al. VPAC receptor mediated tumor cell targeting by protamine based nanoparticles. *J Drug Target*. 2010;18(6):457–467.
44. Parker JC. Transport and distribution of charged macromolecules in lungs. *Adv Microcirc*. 1987(13):150–159.
45. Chono S, Tauchi Y, Morimoto K. Influence of particle size on the distributions of liposomes to atherosclerotic lesions in mice. *Drug Dev Ind Pharm*. 2006;32(1):125–135.
46. Maiseyeu A, Mihai G, Kampfrath T, et al. Gadolinium-containing phosphatidylserine liposomes for molecular imaging of atherosclerosis. *J Lipid Res*. 2009;50(11):2157–2163.
47. Ahsan F, Rivas IP, Khan MA, Torres Suarez AI. Targeting to macrophages: role of physicochemical properties of particulate carriers – liposomes and microspheres – on the phagocytosis by macrophages. *J Control Release*. 2002;79(1–3):29–40.
48. Roser M, Fischer D, Kissel T. Surface-modified biodegradable albumin nano- and microspheres. II: effect of surface charges on in vitro phagocytosis and biodistribution in rats. *Eur J Pharm Biopharm*. 1998;46(3):255–263.
49. Nieuwdorp M, Meuwese MC, Vink H, Hoekstra JB, Kastelein JJ, Stroes ES. The endothelial glycocalyx: a potential barrier between health and vascular disease. *Curr Opin Lipidol*. 2005;16(5):507–511.
50. Plump AS, Breslow JL. Apolipoprotein E and the apolipoprotein E-deficient mouse. *Annu Rev Nutr*. 1995;15:495–518.
51. Swirski FK, Libby P, Aikawa E, et al. Ly-6Chi monocytes dominate hypercholesterolemia-associated monocytosis and give rise to macrophages in atheromata. *J Clin Invest*. 2007;117(1):195–205.
52. Storm G, Crommelin DJ. Liposomes: quo vadis? *Drug Discovery Today*. 1998;1(1):19–31.